Defects of Prostate Development and Reproductive System in the Estrogen Receptor-α Null Male Mice

Ming Chen, Iawen Hsu, Andrew Wolfe, Sally Radovick, KuoHsiang Huang, Shengqiang Yu, Chawnshang Chang, Edward M. Messing, and Shuyuan Yeh

Departments of Urology and Pathology, University of Rochester Medical Center (M.C., I.H., K.H., S.Y., C.C., E.M.M., S.Y.), Rochester, New York 14642; and Department of Pediatrics, Johns Hopkins University College of Medicine (A.W., S.R.), Baltimore, Maryland 21287

The estrogen receptor-α knockout (ERαKO, ER$\alpha^{-/-}$) mice were generated via the Cre-loxP system by mating floxed ERα mice with β-actin (ACTB)-Cre mice. The impact of ERα gene deletion in the male reproductive system was investigated. The ACTB-Cre/ER$\alpha^{-/-}$ male mice are infertile and have lost 90% of epididymal sperm when compared with wild-type mice. Serum testosterone levels in ACTB-Cre/ER$\alpha^{-/-}$ male mice are 2-fold elevated. The ACTB-Cre/ER$\alpha^{-/-}$ testes consist of atrophic and degenerating seminiferous tubules with less cellularity in the disorganized seminiferous epithelia. Furthermore, the ventral and dorsal-lateral prostates of ACTB-Cre/ER$\alpha^{-/-}$ mice display reduced branching morphogenesis. Loss of ERα could also be responsible for the decreased fibroblast proliferation and changes in the stromal content. In addition, we found bone morphogenetic protein, a mesenchymal inhibitor of prostatic branching morphogenesis, is significantly up-regulated in the ACTB-Cre/ER$\alpha^{-/-}$ prostates. Collectively, these results suggest that ERα is required for male fertility, acts through a paracrine mechanism to regulate prostatic branching morphogenesis, and is involved in the proliferation and differentiation of prostatic stromal compartment. (***Endocrinology*** **150: 251–259, 2009)**

Estrogens exert a variety of regulatory functions on growth, development, and differentiation in both the female and male reproductive systems (1). Estrogens actions are mediated by estrogen receptors (ERs) (2–4), encoded by two distinct genes, ERα and ERβ. Although *in vitro* assays have demonstrated that ERα and ERβ have similar DNA and ligand binding properties (5, 6), ERα and ERβ display a variety of differences in terms of tissue distribution, transcriptional activation, and knockout (KO) phenotypes (1, 5, 7). Those studies have suggested that ERα and ERβ might regulate different target genes' expressions and biological functions (4, 8, 9).

The specific roles of estrogens and ERs in the male reproductive system remained elusive until the generation of ER knockout mice (ERKO; ER$^{-/-}$). These studies, conducted with conventional ER$\alpha^{-/-}$ and ER$\beta^{-/-}$ mice, revealed that ERα, but not ERβ, acts as a dominant regulator of estrogen signaling in male fertility, testicular steroidogenesis, and developmental estrogenization of the prostate (10–13). The ERα mutation in the conventional ER$\alpha^{-/-}$ mice, generated by insertion of a Neo cassette into exon II of the mouse ERα gene (designated as neo-ER$\alpha^{-/-}$), might not actually represent a null mutation, because a low amount of 61 kDa chimeric ERα protein is still present in the neo-ER$\alpha^{-/-}$ mice (14–17). The truncated ERα protein, which results from a new ERα transcript through alternative splicing, is a chimeric protein incorporating seven amino acids from the neomycin insert into the N-terminal A/B regions and retains an intact DNA binding domain and ligand binding domain in the neo-ER$\alpha^{-/-}$ mice. This protein lacks activation function-1 transactivation function but still possesses estrogen-dependent transactivation activities (16, 18, 19). We were interested in further characterization of the roles of ERα in the male reproductive system with a special focus on studying the roles in prostate development because a growing body of evidence has suggested that estrogens signaling exerts a direct impact on prostate pathogenesis and cancer and that ERα, but not ERβ, is the critical receptor to mediate prostatic developmental estrogenization,

ISSN Print 0013-7227 ISSN Online 1945-7170
Printed in U.S.A.

doi: 10.1210/en.2008-0044 Received January 10, 2008. Accepted August 20, 2008.
First Published Online August 28, 2008

Abbreviations: ACTB, β-Actin; AP, anterior prostate; AR, androgen receptor; BMP, bone morphogenetic protein; DLP, dorso lateral prostate; E2, 17β-estradiol; ER, estrogen receptor; ERKO, ER knockout; FGF, fibroblast growth factor; IHC, immunohistochemistry; KO, knockout; Shh, Sonic Hedgehog; T, testosterone; VP, ventral prostate; Wt, wild type.

squamous metaplasia, and hormonal carcinogenesis (11, 20, 21). Interestingly, the early histological analyses from neo-ERα$^{-/-}$ male mice concluded that prostates from ERα$^{-/-}$ mice were indistinguishable from wild-type (Wt) littermates (22). We hypothesize the chimeric 61-kDa ERα proteins could mask the prostate phenotypes in neo-ERα$^{-/-}$ male mice.

Recently we and others generated floxed ERα transgenic mice by targeting exon III of the mouse ERα gene (14, 23, 24). By mating floxed ERα mice with β-actin (ACTB)-Cre mice, which express *Cre* recombinase ubiquitously under the control of the β-actin promoter, we developed a complete null ERα mutant (designated as ACTB-ERαKO, ACTB-Cre/ERα$^{-/-}$), in which no remaining ERα protein can be detected (24). In this study, we confirmed and validated several key phenotypes of neo-ERα$^{-/-}$ male mice in the ACTB-Cre/ERα$^{-/-}$ mice, such as infertility, atrophic and degenerating seminiferous tubules, and hypospermic epididymides. Importantly, our newly generated ACTB-Cre/ERα$^{-/-}$ male mice display more homogeneous and severe phenotypes in both testes and epididymides compared with neo-ERα$^{-/-}$ mice. Furthermore, we found that ERα acts through a paracrine mechanism to regulate prostatic branching morphogenesis and is involved in the proliferation and differentiation of prostatic stromal compartment.

Materials and Methods

Animals and genotyping

Floxed ERα mice were generated as previously described (24). The ACTB-Cre/ERα$^{-/-}$ mice were generated by mating the floxed ERα homozygous female mice with ACTB-Cre transgenic male mice. After two generations of mating, ACTB-Cre/ERα$^{-/-}$ mice were developed (Fig. 1B). Genomic DNA was used as a template for PCR genotyping and isolated from tail biopsy as previously described (24). The primers used for ACTB-ERα mutant mice were: P1, 5′-AGGCTTTGTCTCGCTTTCCC-3′, P2, 5′-GATCATTCAGAGAGACAAGAGGAACC-3′ (see Fig. 1A; floxed ERα allele); and *Cre*, sense, 5′-AGGTGTAGAGAAGGCACTTAGC-3′; antisense, 5′-CTAATCGCCATCTTCCAGCAGG-3′. The PCR for the genotyping of ACTB-ERα mutant mice was amplified by the P1, P2, and *Cre* primer mixture. The size of P1-P2 fragments for Wt and KO allele was 741 and 223 bp, respectively. The size of *Cre* fragments was 411 bp. The neo-ERα heterozygote mice were purchased from Jackson Laboratories (Bar Harbor, ME). The generation of neo-ERα$^{-/-}$ and genotyping were previously described (19). All animal procedures were approved by the Animal Care and Use committee of the University of Rochester Medical Center, in accordance with National Institutes of Health guidelines.

Fertility test

Five 9- to 12-wk-old ACTB-Cre/ERα$^{+/+}$ (Wt), ACTB-Cre/ERα$^{+/-}$, and ACTB-Cre/ERα$^{-/-}$ males for each genotype were mated with known fertile females for 16 wk. The number of pups and litters were recorded.

Hormone RIA

All male mice were housed individually for 1 wk before collection of serum for hormone analysis. Serum 17β-estradiol (E2), LH, and FSH measurements were determined by RIA at the Northwestern University P30 Center RIA Core Facility under the direction of Dr. John Levine. National Institute of Diabetes and Digestive and Kidney Diseases antiserum and standards (rLH-RP-3 standard/rLH-S-11 antibody and rFSH-RP-2 standard/rFSH-S-11 antibody) were used for LH and FSH mea-

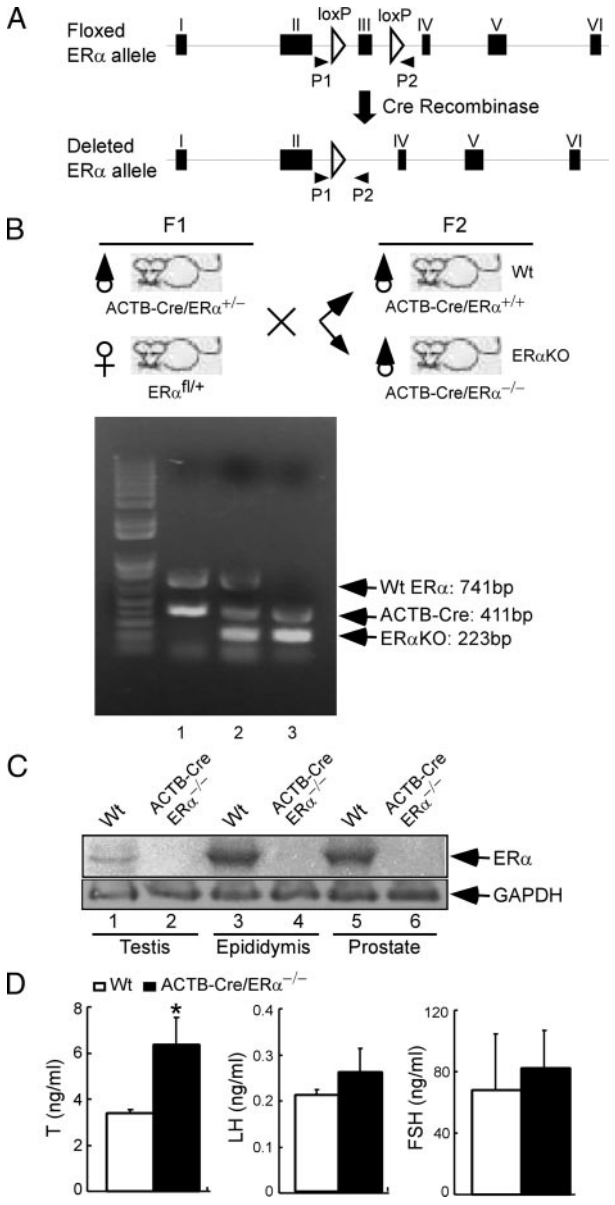

FIG. 1. Breeding and genotyping of ACTB-Cre/ERα$^{-/-}$ male mice via Cre-loxP strategy. A, Using the Cre-loxP strategy, exon III of mouse ERα gene was targeted and flanked by loxP sites. The schematic map shows floxed ERα allele and deleted ERα allele in the ACTB-ERα mutant mice. The primer set, P1 and P2, was used for genotyping. B, Breeding strategy to generate the ACTB-Cre/ERα$^{-/-}$ males and genotyping of ACTB-Cre/ERα$^{-/-}$ males using primer mixture: P1, P2, and *Cre* primer. Floxed ERα homozygous female mice were mated with ACTB-Cre transgenic male mice to obtain ACTB-Cre/ERα$^{+/-}$ male mice (F1). Mating ACTB-Cre/ERα$^{+/-}$ males with floxed ERα heterozygote females obtained the ACTB-Cre/ERα$^{+/+}$ (Wt) and ACTB-Cre/ERα$^{-/-}$ (KO) mice (F2). The genotyping results were as follows: lane 1, ACTB-Cre/ERα$^{+/+}$ mice, and the size of Wt ERα and *Cre* was 741 and 411 bp, respectively; lane 2, ACTB-Cre/ERα$^{+/-}$ mice, in which intervening DNA of floxed ERα allele was deleted by ACTB-Cre recombinase. The size of deleted ERα allele was reduced to 223 bp; lane 3, ACTB-Cre/ERα$^{-/-}$ mice, in which the size of both floxed ERα alleles was reduced to 223 bp by ACTB-Cre recombinase and only the deleted ERα band was present. C, Western blot analysis of ERα protein in the testis, epididymis, and prostate of Wt and ACTB-Cre/ERα$^{-/-}$ males using antibody against ERα C terminus. No ERα immunoreactivity was detected in ACTB-Cre/ERα$^{-/-}$ male reproductive organs (lanes 2, 4, and 6). Glyceraldehyde-3-phosphate dehydrogenase (GAPDH) immunoblotted as an indication of equal loading. D, The serum hormone profiles in the 12- to 14-wk-old ACTB-Cre/ERα$^{-/-}$ males. Results are presented as means ± SD (n = 5). *, $P < 0.05$ *vs.* Wt littermates (statistically significant by Student's unpaired *t* test).

surements. FSH assay sensitivity was 0.05 ng/sample or 1.0 ng/ml. LH assay sensitivity was 0.01 ng/sample or 0.2 ng/ml. An E2 double-antibody RIA kit (Diagnostic Products Corp., Los Angeles, CA) and testosterone (T) double-antibody RIA kit (Diagnostic System Laboratories, Inc., Webster, TX) containing antibodies and standards were used for E2 and T RIAs. Both E2 and T assay sensitivity was at 2.0 pg/ml. Animals used in the hormone studies were approximately 3 months of age.

Tissue dissection and prostatic ductal tips count

Animals were killed by CO_2 asphyxiation. Blood was collected for serum hormone analysis by cardiac puncture. After centrifugation, the serum was frozen at −70 C until assayed. The genital tract of the animals was exposed by a lower abdominal incision. Adipose and connective tissues surrounding the sex organs were gently removed. The individual organs were then microdissected, weighed, photographed, and frozen for further analysis or fixed in Bouin's solution (for testis histology) or formalin (other tissues) for subsequent histological examination. Microdissection of ventral prostate (VP), dorso-lateral prostate (DLP) and anterior prostate (AP) was facilitated by incubating the prostate in the Hanks' buffer containing 1% collagenase for 1 h at 37 C. Further dissection was performed using a dissecting microscope and fine forceps. The number of ductal tips, branches, and branch points was counted.

Sperm counting

The whole mouse epididymis was cut into small pieces in 1.5 ml RPMI 1640 media, incubated for 40 min at 37 C to release the sperm from the tissue, and then diluted to count the sperm numbers per epididymis.

Western blotting

Protein extracts were prepared from the male reproductive tissues of different mouse genotypes as described previously (24). Eighty micrograms of protein were separated on a 10% gel by SDS-PAGE and transferred onto a nitrocellulose membrane. ERα was detected with a rabbit polyclonal antibody against the ERα F domain (MC-20; Santa Cruz Biotechnology, Santa Cruz, CA). The same blot was hybridized with an anti-glyceraldehyde-3-phosphate dehydrogenase antibody as an internal control (0411; Santa Cruz Biotechnology).

Immunohistochemistry (IHC) and immunofluorescent staining

IHC was carried out as described previously (25, 26). Briefly, the paraffin-embedded tissue blocks were cut at 4-mm thickness, dewaxed, and rehydrated. Antigens were retrieved by boiling in 10 mM citrate buffer (pH 7.0) for 15 min. The sections were incubated in 1% H_2O_2 in PBS for 30 min at room temperature to quench endogenous peroxidase. To block nonspecific binding, sections were incubated in 5% normal serum prepared from the host of secondary antibodies for 1 h at 4 C. Sections were incubated with the following antibodies and dilutions: anti-Ki-67 (NCL-Ki-67p, 1:1000), anti-androgen receptor (N-20, 1:400), anti-ERβ (PA1–310B, 1: 50), anti-vimentin (LN-6, 1:200), and anti-desmin (DE-U-10, 1:300) in 3% BSA in PBS overnight at 4 C. For IHC, the tissue slides were then incubated with 1:300 diluted biotinylated secondary antibody (Vector Laboratories, Burlingame, CA) and ABC solution (Vector Laboratories) and then stained using AEC (Dako, Carpenteria, CA), and Mayer's hematoxylin counterstaining. Negative controls were incubated without primary antibody. For immunofluorescent staining, the tissue slides were incubated with 1:100 Texas red-conjugated goat anti-mouse IgG and fluorescein isothiocyanate-conjugated goat anti-rabbit IgG (ICN, Costa Mesa, CA). Stained slides were mounted with mounting media containing 4′,6′-diamino-2-phenylindole and visualized with a fluorescent microscope. The ratio of Ki-67-positive to total nuclei was calculated in at least 500 cells examined in each of three randomly selected regions. The data were expressed as a percentage of Ki-67 positive cells.

RNA extraction, RT-PCR, and quantitative real-time PCR

Total RNA was extracted and purified using Trizol (Invitrogen, Carlsbad, CA) according to the manufacturer's instructions. RT-PCR has been described previously (27). Briefly, 3 μg total RNA were subjected to reverse transcription using Superscript III (Invitrogen). The real-time PCR was performed with first-strand cDNA, specific gene primers, and SYBR Green PCR master mix (Bio-Rad, Hercules, CA). The PCR cycle was performed as follows: 94 C for 3 min, 40 cycles of 94 C for 30 sec, 60 C for 30 sec, and 72 C for 30 sec on an iCycler iQ multicolor real-time PCR detection system (Bio-Rad). Primer sequences were as follows: vimentin, sense, 5′-CGGCTGCGAGAGAAATTGC-3′; antisense, 5′-CCACTTTCCGTTCAAGGTCAAG-3′; desmin, sense, 5′-AGCAGGAGATGATGGAATAC-3′; antisense, 5′-CGGAAGTTGAGAGCAGAG-3′; smooth muscle α-actin, sense, 5′-GCCAACAAGGGTCCATCC-3′; antisense, 5′-CACCATTCTTCAGCCACAC-3′; fibroblast growth factor (FGF)-2: sense, 5′-AACGGCGGCTTCTTCCTG-3′; antisense, 5′-TGGCACACACTCCCTTGATAG-3′. FGF7, sense, 5′-TCCTGCCAACTCTGCTCTAC-3′; antisense, 5′-CTTTCACTTTGCCTCGTTTGTC-3′. FGF10, sense, 5′-CTGCTGTTGCTGCTTCTTG-3′; antisense, 5′-TGACCTTGCCGTTCTTCTC-3′. Sonic hedgehog (Shh), sense, 5′-AATGCCTTGGCCATCTCTGT-3′; antisense, 5′-GCTCGACCCTCATAGTGTAGAGACT-3′. bone morphogenetic protein (BMP)-4, sense, 5′-GGTGTGGATGCCGCTGAG-3′; antisense, 5′-GGTATGTGTAGGTGGTTGAATGG-3′. BMP7, sense, 5′-GAAGTCCATCTCCGTAGTATCCG-3′; antisense, 5′-TCACAGTAGTAGGCAGCATAGC-3′. 18S, sense, 5′-TGCCTTCCTTGGATGTGGTAG-3′; antisense, 5′-CGTCTGCCCTATCAACTTTCG-3′. Each sample was run in triplicate. Data were analyzed using iCycler iQ software (Bio-Rad).

Results

Generation and genotyping of ACTB-Cre/ERα$^{-/-}$ male mice

To use a Cre-loxP conditional KO strategy, we generated a floxed ERα mouse in which exon III of ERα is flanked by two loxP sites (Fig. 1A). Deletion of exon III in the floxed ERα allele by Cre-mediated recombination resulted in a premature stop codon at the new amino acid 158 due to the splicing of exons II and IV.

The ACTB-Cre/ERα$^{-/-}$ mice were generated by mating floxed ERα female mice with ACTB-Cre transgenic male mice. After two generations of mating, ACTB-Cre/ERα$^{-/-}$ male mice and Wt littermates were developed (Fig. 1B). Western blotting showed that no ERα polypeptide is present in the ACTB-Cre/ERα$^{-/-}$ testis, epididymis, and prostate immunoreacting with an antibody directed against ERα F domain, which is consistent with our previous studies demonstrating that our newly generated ACTB-Cre/ERα$^{-/-}$ mice are complete ERα null mutants (Fig. 1C) (24).

Serum hormone profiles in ACTB-Cre/ERα$^{-/-}$ males

Serum T levels of ACTB-Cre/ERα$^{-/-}$ male mice were around 2-fold higher than those of Wt littermates (Fig. 1D, 6.35 ± 1.19 *vs.* 3.38 ± 0.16, $P < 0.05$), which is consistent with higher serum T levels in the neo-ERα$^{-/-}$ mice (1, 13). Both FSH and LH levels were slightly higher in ACTB-Cre/ERα$^{-/-}$ male mice than in Wt littermates (Fig. 1D); however, the difference was not statistically significant. There was no difference in the E2 level between male

TABLE 1. Fertility test of ERα Wt and mutant males

Genotype	n	Litters	Pups	Pups per litter	Litters per male
Wt	5	15	129	8.6 ± 1.55	3.0 ± 0.7
ACTB-Cre/ERα$^{+/-}$	5	14	125	8.9 ± 1.38	2.8 ± 0.4
ACTB-Cre/ERα$^{-/-}$	5	0	0	0	0

Eight- to 12-wk-old male mice were bred with known fertile females for 16 wk. Results are presented as means ± SD.

ACTB-Cre/ERα$^{-/-}$ and Wt littermates. All of them had baseline E2 levels (2 pg/ml) at the sensitivity of the assay (data not shown).

Infertility and severe genital tract phenotype in adult ACTB-Cre/ERα$^{-/-}$ male mice

ACTB-Cre/ERα$^{-/-}$ male mice were infertile after 16 wk of continuous mating tests (Table 1), which is consistent with the male infertility in other ERα$^{-/-}$ studies (13, 14). Meanwhile, we found ACTB-Cre/ERα$^{+/-}$ mice have normal fertility compared with Wt littermates, indicating that haploid expression of the ERα gene is capable of maintaining normal fertility. Comparing 3-month-old ACTB-Cre/ERα$^{-/-}$ to Wt male mice, the size of ACTB-Cre/ERα$^{-/-}$ testes was smaller than that of Wt testes (Fig. 2A). The weight of ACTB-Cre/ERα$^{-/-}$ testes was significantly less than that of Wt testes (Fig. 2B). ACTB-Cre/ERα$^{-/-}$ seminal vesicles were slightly heavier than those of Wt littermates (Fig. 2B), which might be due to the stimulation by the higher serum T levels in the ACTB-Cre/ERα$^{-/-}$ mice. Both the size and weight of ACTB-Cre/ERα$^{-/-}$ epididymides were slightly lower than those of Wt littermates.

Histological analyses demonstrated that ACTB-Cre/ERα$^{-/-}$ testes consisted of atrophic and degenerating seminiferous tubules with disorganized seminiferous epithelia (Fig. 3A). The seminiferous epithelial layer contained few spermatogenic cells with decreased germ cell number (Fig. 3A). The vacuoles were often present in the seminiferous epithelial layer (Fig. 3A, IV, *arrowheads*). The phenotypes in the ACTB-Cre/ERα$^{-/-}$ testes were consistent with previous studies in the neo-ERα$^{-/-}$ (13); however, the above phenotypes in the neo-ERα$^{-/-}$ testes tended to be heterogeneous (13), in which some seminiferous tubules seemed to be normally developed (Fig. 3B, *arrows*). In contrast, the defective seminiferous tubules appeared to be widely distributed and homogeneous in the ACTB-Cre/ERα$^{-/-}$ testes (Fig. 3A). The adult ACTB-Cre/ERα$^{-/-}$ epididymides were hypospermic compared with Wt as indicated by the pale staining of the epididymal lumen (Fig. 3C). The hypospermic phenotype is homogeneous and consistent in the ACTB-Cre/ERα$^{-/-}$ epididymides. However, the hypospermic epididymides in the neo-ERα$^{-/-}$ mice were heterogeneous and some epididymal lumens contained levels of sperm comparable with Wt mice (Fig. 3C, *arrows*). Furthermore, comparing the sperm count in 3-month-old mice, we found that the sperm number in ACTB-Cre/ERα$^{-/-}$ epididymides was only 10% of that in Wt littermates (Fig. 2C). Compared with the conventional neo-ERα$^{-/-}$ mice, those results demonstrated that the ACTB-Cre/ERα$^{-/-}$ mouse line displays a more homogeneous phenotype and represents an improved ERαKO mouse model for the study of ERα function in the male reproductive system.

Reduced branching morphogenesis in the VP and DLP of ACTB-Cre/ERα$^{-/-}$ males

A growing body of evidence has suggested that estrogen signaling exerts a direct impact on prostate pathogenesis and cancer. Paradoxically, the previous reports concluded that prostates from neo-ERα$^{-/-}$ mice were histologically indistinguishable from Wt littermates (14, 22). Because we established an improved ERαKO mouse model, we went further to investigate different prostate developmental processes including prostate growth, branching morphogenesis, cell proliferation, and gene regulation. After microdissection of ACTB-Cre/ERα$^{-/-}$ prostates, there was no significant difference in the weights of each prostatic lobe between adult Wt and ACTB-Cre/ERα$^{-/-}$ male mice (supplemental Fig. 1, published as supplemental data on

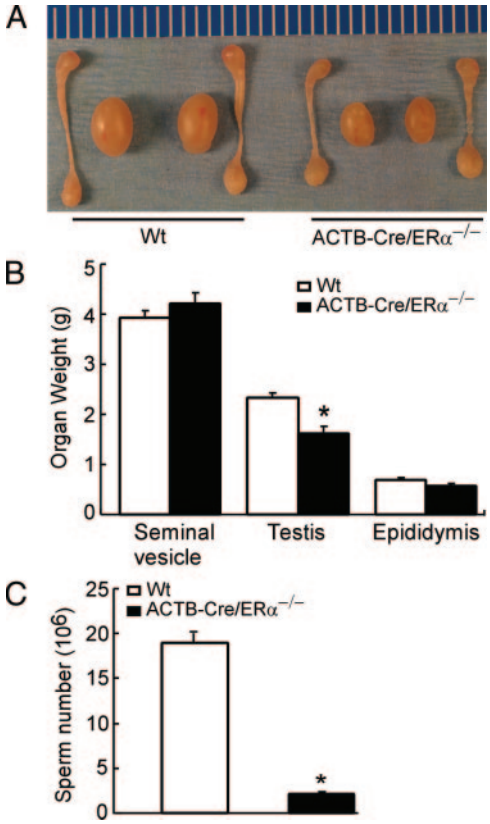

FIG. 2. The male reproductive organ in the 12-wk-old Wt and ACTB-Cre/ERα$^{-/-}$ males. A, The comparison of the anatomy of the genital tracts between adult ACTB-Cre/ERα$^{-/-}$ and Wt littermates. B, The comparison of the reproductive organ weights between adult ACTB-Cre/ERα$^{-/-}$ and Wt littermates. The organs from 12-wk-old males were weighed. *, $P < 0.05$ *vs.* Wt littermates (statistically significant by Student's unpaired *t* test). Results are means ± SD (n = 8). C, The comparison of the sperm count between adult ACTB-Cre/ERα$^{-/-}$ and Wt littermates. *, $P < 0.01$ *vs.* Wt littermates (statistically significant by Student's unpaired *t* test). Results are means ± SD (n = 3).

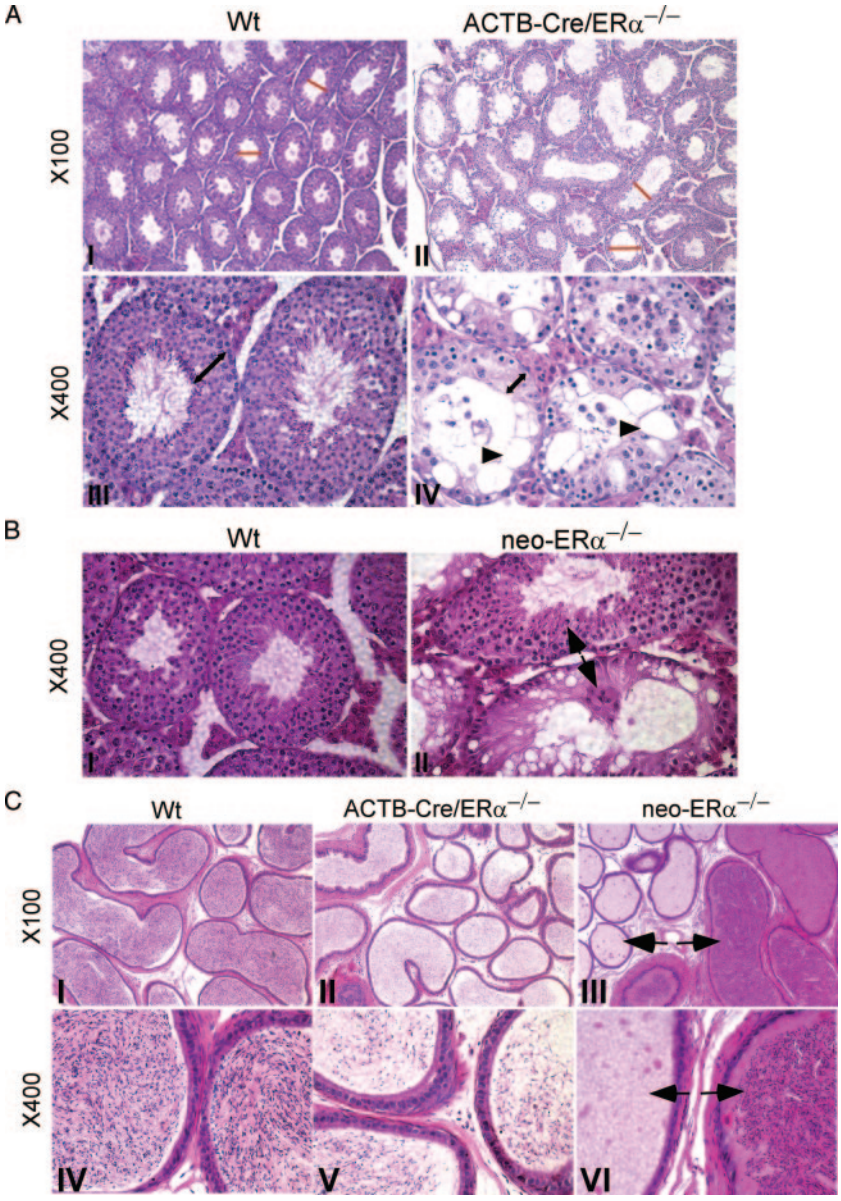

FIG. 3. Histological analyses and comparison of testes and epididymides in the 12-wk-old Wt, neo-ERα$^{-/-}$, and ACTB-Cre/ERα$^{-/-}$ males. A, Histological analyses of testes from Wt and ACTB-Cre/ERα$^{-/-}$ males. The adult Wt testes consist of compact seminiferous tubules (I and III). The adult ACTB-Cre/ERα$^{-/-}$ testes consist of atrophic and degenerating seminiferous tubules (*red line*) (II). The seminiferous epithelial layer in the ACTB-Cre/ERα$^{-/-}$ testes contained few spermatogenic cells with decreased germ cell number compared with Wt (IV *vs.* III, *double-headed arrows*), and the vacuoles were often present in the seminiferous epithelial layer (IV, *arrowhead*). B, Histological analyses of testes from Wt and neo-ERα$^{-/-}$ males. The adult neo-ERα$^{-/-}$ testes showed the defects with less extent compared with ACTB-Cre/ERα$^{-/-}$ testes. Some normal seminiferous tubules could be observed in neo-ERα$^{-/-}$ testes (II, *arrow*). C, Histological analyses of caudal epididymis from Wt, ACTB-Cre/ERα$^{-/-}$, and neo-ERα$^{-/-}$ males. The adult Wt epididymis is full of sperm in the caudal lumen (I and IV). The caudal epididymis in the adult ACTB-Cre/ERα$^{-/-}$ males contains much less sperm and appears pale in the histology staining (II and V). The epididymis in the adult neo-ERα$^{-/-}$ males exhibits the heterogeneous phenotype. Some epididymal tubes contain very few sperm, but some are full of sperm (III and VI, *arrows*).

The Endocrine Society's Journals Online web site at http://endo.endojournals.org). After removing the stromal compartment by partial enzyme digestion, we found there were significant differences in branching morphogenesis between adult ACTB-Cre/ERα$^{-/-}$ and Wt prostates (Fig. 4A). Three parameters of branching morphogenesis were quantified in individual lobes of adult mice, including ductal tips, branches, and points. Each of the three parameters derived from prostatic branching showed significantly decreased numbers in both ACTB-Cre/ERα$^{-/-}$ VP and DLP compared with Wt mice, which indicated prostatic branching morphogenesis in ACTB-Cre/ERα$^{-/-}$ mice was reduced (Fig. 4B). We did not observe a difference in the branching morphogenesis of the AP between ACTB-Cre/ERα$^{-/-}$ and Wt mice, which could be due to the different embryological origin of the AP *vs.* the VP and DLP (28). These results suggest that ERα is involved in prostatic branching morphogenesis.

Decreased fibroblast proliferation and changes in the stromal content in the ACTB-Cre/ERα$^{-/-}$ prostates

The mouse prostate undergoes extensive branching morphogenesis during the first 15 d of life (29), which suggests that cell proliferation is highest during these neonatal stages. Because we observed reduced branching morphogenesis, we were interested in comparing the proliferation activity of the VP between ACTB-Cre/ERα$^{-/-}$ and Wt mice at 1 wk of age (Fig. 4C). Ki-67 positive staining showed that there was no difference in epithelial proliferation of the VP between ACTB-Cre/ERα$^{-/-}$ and Wt littermates (Fig. 4, C, *arrows*, and D, 3.53 ± 0.46 *vs.* 3.58 ± 0.52%); however, there was a significant difference in stromal proliferation of the VP between ACTB-Cre/ERα$^{-/-}$ and Wt littermates (Fig. 4, C, *arrowheads*, and D, 1.17 ± 0.29 *vs.* 2.1 ± 0.36%). Due to the low homeostasis rate in the adult prostate, both epithelial and stromal cell proliferation was very rare; the proliferation difference was not observed in the adult ACTB-Cre/ERα$^{-/-}$ and Wt littermates (data not shown).

The decreased stromal cell proliferation in the neonatal ACTB-Cre/ERα$^{-/-}$ prostates could potentially influence the stromal cellular composition and differentiation. Early studies with estrogenized rat prostates demonstrated that the periductal fibroblasts, but not smooth muscle cells, have active proliferation in response to estrogens exposure (30). To determine which cell types in the stromal compartment proliferate, we performed immunofluorescence analyses for neonatal VP stromal cells.

The stromal compartment in the mouse prostate mainly consists of periductal smooth muscle cells, which are the important mediators of androgen signaling for prostatic epithelial bud growth and differentiation (Fig. 4E, j and n) (31), and fibroblasts distributed in the interductal spaces between epithelial ducts

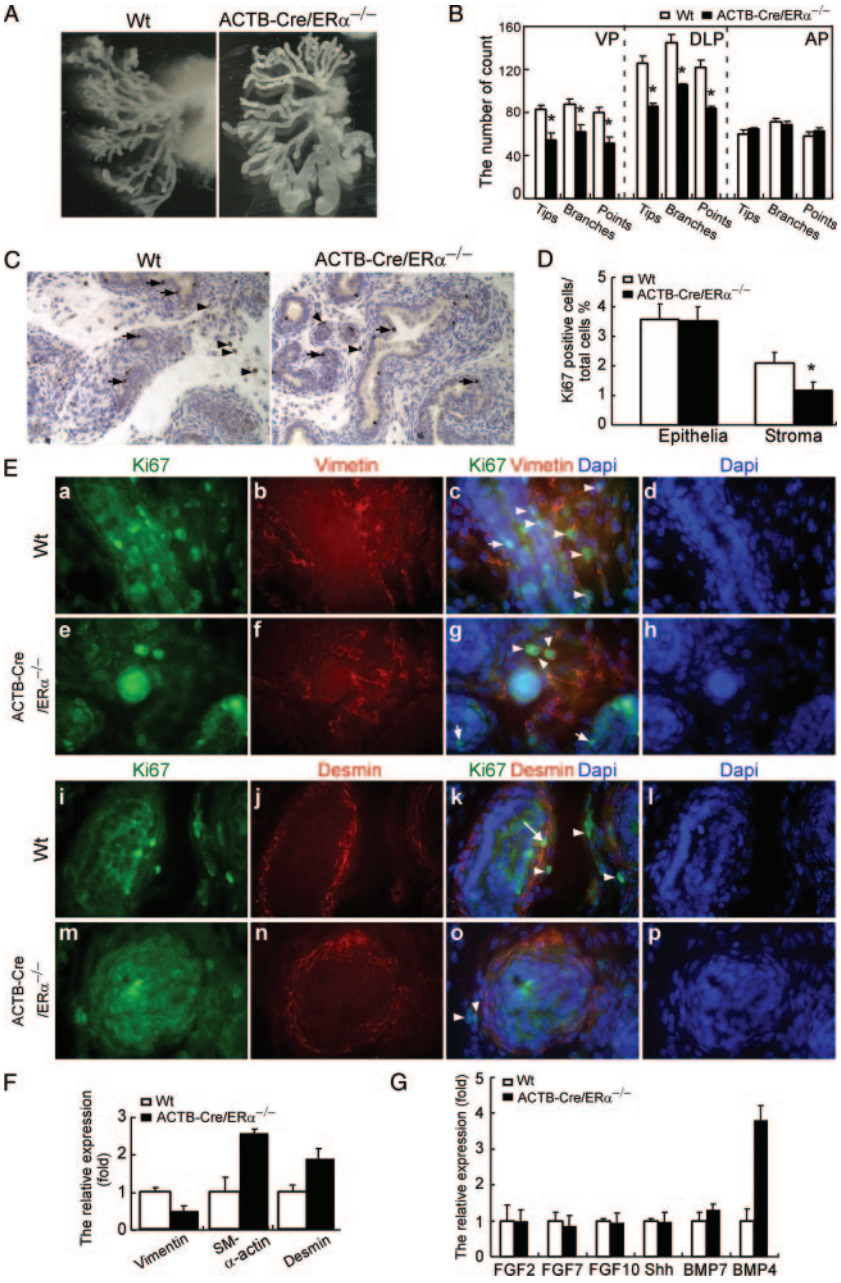

FIG. 4. The defects of prostate development in the ACTB-Cre/ERα$^{-/-}$ males. A, Photographs demonstrating the branching morphogenesis from a representative pair of adult ACTB-Cre/ERα$^{-/-}$ and Wt littermates after microdissection of VP. B, The total number of ductal tips, branches, and ductal points in ACTB-Cre/ERα$^{-/-}$ and Wt littermates. The VP and DLP, but not AP, of ACTB-Cre/ERα$^{-/-}$ mice have significantly fewer ductal tips than those of WT littermates. *, $P < 0.01$ *vs.* Wt littermates (statistically significant by Student's unpaired *t* test). Results are means ± SD (n = 5). C and D, The cell proliferation of VP from 1-wk-old ACTB-Cre/ERα$^{-/-}$ and Wt littermate is determined by Ki-67 immunostaining (C). *Arrows* show positive staining in the epithelial cells. *Arrowheads* show positive staining in the stromal cells. The Ki-67 proliferation index is scored as the percentage of Ki-67-positive cells (D). Note that there was significantly reduced stromal proliferation in the ACTB-Cre/ERα$^{-/-}$ VP. *, $P < 0.05$, compared with Wt VP cell proliferation, Student's *t* test. The results are means ± SD of triplicate samples. E, Characterization of proliferating stromal cells in the ACTB-Cre/ERα$^{-/-}$ and Wt VP. Immunofluorescence analyses were carried out by using sections from neonatal VP lobes. Each section was double stained by Ki-67 and vimentin (fibroblast cell marker) or desmin (smooth muscle cell marker) followed by counterstaining with 4′,6′-diamino-2-phenylindole (DAPI) to visualize the nuclei. *Arrowheads* show positive Ki-67 staining in the fibroblasts (c, g, k, and o). *Arrows* show positive Ki-67 staining in the epithelial cells (c and g). *Long arrow* shows positive Ki-67 staining in the smooth muscle cells (k). Note the fibroblasts are actively proliferating (c and g), but the smooth muscle cells rarely proliferate (k and o) in the stromal compartment. F, The comparison of the expression of the stromal marker between ACTB-Cre/ERα$^{-/-}$ and Wt littermates by real-time PCR. Assays were performed on RNA from the VP of each individual mouse and then averaged for the gene expression. 18s acts as internal control. The results are means ± SD of six samples. Note that the expression of vimentin is (Fig. 4E, b and f). The dual-immunofluorescence analyses were done using vimentin as the fibroblast marker and desmin as the smooth muscle cell marker costaining with Ki-67. Our analysis showed that the fibroblasts are the predominantly proliferating stromal cells in the neonatal stromal compartment in the VP of both ACTB-Cre/ERα$^{-/-}$ and Wt littermates (Fig. 4E, *arrowheads*). The smooth muscle cells are largely Ki-67 negative and proliferate rarely (Fig. 4E, k and o). Occasionally the proliferating smooth muscle cells can also be observed in the VP of neonatal Wt (Fig 4E, k, *long arrow*) and ACTB-Cre/ERα$^{-/-}$ mice (data not shown). Consistent with previous IHC staining, the immunofluorescence results also showed the decreased cell proliferation in ACTB-Cre/ERα$^{-/-}$ stromal cells. To examine whether decreased fibroblast proliferation would affect stromal composition in the ACTB-Cre/ERα$^{-/-}$ prostate, we applied real-time PCR to detect the expression of fibroblast and smooth muscle cellular markers including vimentin, smooth muscle α-actin, and desmin. As shown in Fig. 4F, there was more than a 50% decrease in the expression of vimentin in the ACTB-Cre/ERα$^{-/-}$ prostates compared with Wt littermates, which is consistent with our observation that ACTB-Cre/ERα$^{-/-}$ prostates have decreased fibroblast cell proliferation. In addition, we also observed that there was a 2- to 3-fold increase in the expression of smooth muscle markers, smooth muscle α-actin and desmin, in the ACTB-Cre/ERα$^{-/-}$ prostates. Taken together, these results indicated that loss of ERα in the mouse prostate would lead to decreased fibroblast cell proliferation and content, but increased smooth muscle cell content, which suggested that ERα could be involved in prostatic stromal cellular proliferation and differentiation.

Increased BMP4 expression, but not BMP7, in the ACTB-Cre/ERα$^{-/-}$ prostates

The interaction between prostate epithelial and mesenchymal cells necessary for prostatic branching morphogenesis is regulated by the time- and region-specific expression of signaling molecules (32). To determine which molecules might be regulated by ERα in the mouse prostate to influence the branching morphogenesis, we examined the expression of several important genes involved in prostatic branching morphogenesis, including Shh, the FGF family, BMP4, and BMP7 by real-time PCR.

Our results showed that only the expression of BMP4 was significantly and selectively up-regulated in the VP of adult ACTB-Cre/ER$\alpha^{-/-}$ male mice (Fig. 4G), not that of Shh, FGF2, FGF7, FGF10, or BMP7. Among these factors, BMP4 and BMP7 are known to inhibit prostatic branching morphogenesis, and BMP4 is exclusively expressed in the prostatic stromal cells (33, 34). Collectively our studies indicated ERα might act through a paracrine mechanism to regulate prostatic branching morphogenesis. Both decreased stromal proliferation (Fig. 4, C and D) and up-regulation of BMP4 (Fig. 4G) could contribute to the reduced branching morphogenesis in ACTB-Cre/ER$\alpha^{-/-}$ prostates. Those observations have not been reported in the other ER$\alpha^{-/-}$ mouse models.

Discussion

To generate our ER$\alpha^{-/-}$ mouse model, we targeted exon III of the mouse ERα gene, which encodes the first zinc finger of the ERα-DNA binding domain and plays an important role for ER-estrogen response element binding and genomic regulation of ERα target genes (1). Deletion of ERα exon III will result in a premature stop codon at the new amino acid 158 due to the splicing of exon II and IV. However, by Western blotting, we could not detect any ERα polypeptide immunoreacting with either ERα-N-terminal antibody or ERα-C-terminal antibody in our ACTB-Cre/ER$\alpha^{-/-}$ uterus extract; these results demonstrate that our newly generated ACTB-Cre/ER$\alpha^{-/-}$ mice are complete ERα null mutants (24). In contrast, the previously generated neo-ER$\alpha^{-/-}$ mice not only express a 46-kDa ERα Δ1 protein, but also a 61-kDa E1 chimeric protein. This E1 protein lacks activation function-1 transactivation function, but still possesses estrogen-dependent transactivation activities (18, 19). We also examined the expression of ERα in male reproductive organs including the testis, epididymis, and prostate in ACTB-Cre/ER$\alpha^{-/-}$ mice using the ERα-C-terminal antibody. Consistent with ACTB-Cre/ER$\alpha^{-/-}$ females, there is no ERα protein detectable in ACTB-Cre/ER$\alpha^{-/-}$ mouse tissue. Therefore, the changes reported herein regarding the male reproductive system are the result of deletion of functional ERα protein.

ACTB-Cre/ER$\alpha^{-/-}$ males were infertile, which agreed with other ER$\alpha^{-/-}$ studies (14, 22). Detailed histological analyses showed that ACTB-Cre/ER$\alpha^{-/-}$ male mice displayed severe phenotypes in the genital tract indicated by more homogeneous phenotypes in both testes and epididymides compared with neo-ER$\alpha^{-/-}$ mice. Because we plan to characterize *in vivo* roles of ERα in the reproductive system with respect to the tissue and temporal-specific effects and their target genes, findings in the ACTB-Cre/ER$\alpha^{-/-}$ male mice provided strong evidence that our floxed ERα mouse line represents an appropriate mouse model to generate tissue-specific ERαKO mice in the future.

A growing body of evidence has suggested that estrogen signaling exerts a direct impact on prostate pathogenesis and cancer. ERα, but not ERβ, is the critical receptor to mediate prostatic developmental estrogenization, squamous metaplasia, and hormone carcinogenesis (11, 20, 21). The studies from neo-ER$\alpha^{-/-}$ mice concluded that prostates from ER$\alpha^{-/-}$ mice were indistinguishable from Wt littermates by histological analyses (22). However, the remaining 61-kDa E1 chimeric protein might compromise this conclusion. We went further to investigate different prostate developmental processes including branching morphogenesis, cell proliferation, and gene regulation.

The rodent prostate is rudimentary at birth, and most (70%) of the ductal branching morphogenesis of mouse prostate occurs during the first 15 d of postnatal life (29). Neonatal prostatic ductal morphogenesis may occur in the absence of T; however, the full development of prostatic branching morphogenesis requires several different pathways/influences, including T/androgen receptor (AR), ERα, and others (35). Our studies showed that the VP and DLP of ACTB-Cre/ER$\alpha^{-/-}$ male mice had reduced branching morphogenesis, which suggested that ERα is involved in prostatic branching morphogenesis. We did not observe the difference in the branching morphogenesis of AP between ACTB-Cre/ER$\alpha^{-/-}$ and Wt mice, which could be due to the difference in the embryological origin of the AP *vs.* the VP and DLP. The VP and DLP develop from endodermal urogenital sinus and are embryologically homologous to human prostate (2), but the AP develops from the urogenital sinus epithelium and seminal vesicle mesenchyme. Therefore, it is possible that the regulation of the branching morphogenesis of the AP might be different from that of the VP and DLP and is less dependent on ERα functions.

The prostate is primarily considered to be an androgen target organ. Higher doses of estrogens permanently suppress the neonatal rat or mouse prostate growth and prostatic branching morphogenesis by reducing T production, suppressing AR expression and inducing prostatic epithelial regression (36–40). Therefore, the effect of higher doses of estrogens on mouse prostate might not be due to the roles of ERs in the mouse prostate development. Recent studies by Taylor *et al.* (40) demonstrated that the effects of higher doses of estrogens were able to cause reduced AR expression and induce prostatic epithelial cell apoptosis in the wild-type, αERKO, and βERKO prostates and further suggested that the effects of higher doses of estrogens were independent of ERs and did not reflect the *in vivo* ERs function. In contrast, the levels of AR expression were not altered in the ACTB-Cre/ER$\alpha^{-/-}$ prostates, even though ACTB-Cre/ER$\alpha^{-/-}$ males have 2-fold higher systemic T levels (supplemental Fig. 2), which suggest that the defects in the ACTB-Cre/ER$\alpha^{-/-}$ prostates could be directly due to the loss of ERα and are not compromised by the AR effect. Several studies in which neonatal mice and rats were exposed to low doses of estrogens have reported an increase in AR expression, prostate weight, and prostatic budding (41, 42), which suggest that the physiological range of es-

decreased, but the expression of both smooth muscle α-actin and desmin is increased in the ACTB-Cre/ER$\alpha^{-/-}$ VP. G, The comparison of the expression levels of the genes involved in prostatic branching morphogenesis between ACTB-Cre/ER$\alpha^{-/-}$ and Wt littermates by real-time PCR. Assays were performed on RNA from the VP of each individual mouse and then averaged for the gene expression. 18s acts as internal control. The results are means $\pm$ SD of six samples. *, $P < 0.05$, compared with Wt gene expression, Student's *t* test. Note that only BMP4 is significantly up-regulated in the ACTB-Cre/ER$\alpha^{-/-}$ VP.

trogens might promote prostatic branching morphogenesis and is consistent with our current findings.

Branching morphogenesis is a coordinated growth of both prostatic epithelial and stromal cells. By examining proliferation activity in the neonatal prostate, we also found that fibroblast cell proliferation was significantly reduced in the ACTB-Cre/ERα$^{-/-}$ prostates of 1-wk-old pups, which could partly contribute to the limited branching in the ACTB-Cre/ERα$^{-/-}$ prostates. Because epithelial ERβ has been reported to elicit an antiproliferative effect in the mouse prostate (43), the decreased prostatic fibroblast proliferation may be indirectly mediated through alteration of epithelial ERβ; however, we did not observe any change in the expression and cellular distribution of ERβ in ACTB-Cre/ERα$^{-/-}$ prostates (supplemental Fig. 3). ERα is expressed in both prostatic fibroblasts and smooth muscle cells (30, 44). Administration of estrogens has been shown to influence both fibroblast and smooth muscle cell proliferation and differentiation (30, 36). In the current studies, loss of ERα in the mouse prostate led to decreased fibroblast cell proliferation and content but increased smooth muscle cell content, which suggested that ERα could have a differential effect on the two types of stromal cells and potentially be involved in the remodeling of prostate stromal cellular composition.

Stromal-epithelial interaction plays an important role in normal prostatic development and carcinogenesis. A series of reciprocal paracrine signals between the prostatic epithelium and stroma that are essential for regulating branching morphogenesis include the Shh, FGF family, and BMP family. We found the selective up-regulation of the expression of BMP4, but not BMP7, in the adult ACTB-Cre/ERα$^{-/-}$ prostates. Because BMP4 is a mesenchymal factor that inhibits prostatic branching morphogenesis (34), the up-regulation of BMP4 in the ACTB-Cre/ERα$^{-/-}$ prostates could directly contribute to the reduced branching morphogenesis. How ERα suppresses BMP4 expression and regulates the BMP4 activity *in vivo* in the prostatic stromal cells remains to be elucidated. Further studies are needed to determine the regulatory mechanism of ERα in BMP4's expression.

In conclusion, we have generated an ERαKO mouse model in which exon III of the ERα has been deleted. We have characterized the functions of ERα in the male genital tract and prostate using our ERα$^{-/-}$ mouse model. The current studies in ACTB-Cre/ERα$^{-/-}$ mice have extended previous ERα$^{-/-}$ research and have led to new observations in terms of the functions of ERα in normal prostate development. Specifically, our newly generated ACTB-Cre/ERα$^{-/-}$ male mice displayed more homogeneous and severe phenotypes in both testes and epididymides compared with the conventional neo-ERα$^{-/-}$ mice. As the result of complete deletion of ERα, we demonstrated that ACTB-Cre/ERα$^{-/-}$ prostates had reduced branching morphogenesis. Loss of ERα resulted in the up-regulation of BMP4, a mesenchymal inhibitor of prostatic branching morphogenesis, which suggested that ERα might act through a paracrine mechanism to regulate prostatic branching morphogenesis. Importantly, ERα was also found to be necessary to maintain fibroblast proliferation in the prostatic stromal compartment and is involved in remodeling prostatic stromal cellular composition.

Acknowledgments

We thank Brigitte Mann and the Northwestern University RIA Core for hormone measurements and Karen Wolf and Susan R. Schoen for manuscript preparation.

Address all correspondence and requests for reprints to: Dr. Shuyuan Yeh, Department of Urology, University of Rochester Medical Center, 601 Elmwood Avenue, Box 656, Rochester, New York 14642. E-mail: shuyuan_yeh@urmc.rochester.edu.

Disclosure Statement: None of the authors have anything to declare.

References

1. **Couse JF, Korach KS** 1999 Estrogen receptor null mice: what have we learned and where will they lead us? Endocr Rev 20:358–417
2. **Liu MM, Albanese C, Anderson CM, Hilty K, Webb P, Uht RM, Price Jr RH, Pestell RG, Kushner PJ** 2002 Opposing action of estrogen receptors α and β on cyclin D1 gene expression. J Biol Chem 277:24353–24360
3. **Lazennec G, Bresson D, Lucas A, Chauveau C, Vignon F** 2001 ER β inhibits proliferation and invasion of breast cancer cells. Endocrinology 142: 4120–4130
4. **Paech K, Webb P, Kuiper GG, Nilsson S, Gustafsson J, Kushner PJ, Scanlan TS** 1997 Differential ligand activation of estrogen receptors ERα and ERβ at AP1 sites. Science 277:1508–1510
5. **Kuiper GG, Carlsson B, Grandien K, Enmark E, Haggblad J, Nilsson S, Gustafsson JA** 1997 Comparison of the ligand binding specificity and transcript tissue distribution of estrogen receptors α and β. Endocrinology 138: 863–870
6. **Pace P, Taylor J, Suntharalingam S, Coombes RC, Ali S** 1997 Human estrogen receptor β binds DNA in a manner similar to and dimerizes with estrogen receptor α. J Biol Chem 272:25832–25838
7. **Kushner PJ, Agard DA, Greene GL, Scanlan TS, Shiau AK, Uht RM, Webb P** 2000 Estrogen receptor pathways to AP-1. J Steroid Biochem Mol Biol 74: 311–317
8. **Kian Tee M, Rogatsky I, Tzagarakis-Foster C, Cvoro A, An J, Christy RJ, Yamamoto KR, Leitman DC** 2004 Estradiol and selective estrogen receptor modulators differentially regulate target genes with estrogen receptors α and β. Mol Biol Cell 15:1262–1272
9. **Chang EC, Frasor J, Komm B, Katzenellenbogen BS** 2006 Impact of estrogen receptor β on gene networks regulated by estrogen receptor α in breast cancer cells. Endocrinology 147:4831–4842
10. **Krege JH, Hodgin JB, Couse JF, Enmark E, Warner M, Mahler JF, Sar M, Korach KS, Gustafsson JA, Smithies O** 1998 Generation and reproductive phenotypes of mice lacking estrogen receptor β. Proc Natl Acad Sci USA 95: 15677–15682
11. **Prins GS, Birch L, Couse JF, Choi I, Katzenellenbogen B, Korach KS** 2001 Estrogen imprinting of the developing prostate gland is mediated through stromal estrogen receptor α: studies with αERKO and βERKO mice. Cancer Res 61:6089–6097
12. **Akingbemi BT, Ge R, Rosenfeld CS, Newton LG, Hardy DO, Catterall JF, Lubahn DB, Korach KS, Hardy MP** 2003 Estrogen receptor-α gene deficiency enhances androgen biosynthesis in the mouse Leydig cell. Endocrinology 144:84–93
13. **Eddy EM, Washburn TF, Bunch DO, Goulding EH, Gladen BC, Lubahn DB, Korach KS** 1996 Targeted disruption of the estrogen receptor gene in male mice causes alteration of spermatogenesis and infertility. Endocrinology 137:4796–4805
14. **Dupont S, Krust A, Gansmuller A, Dierich A, Chambon P, Mark M** 2000 Effect of single and compound knockouts of estrogen receptors α (ERα) and β (ERβ) on mouse reproductive phenotypes. Development 127:4277–4291
15. **Sims NA, Dupont S, Krust A, Clement-Lacroix P, Minet D, Resche-Rigon M, Gaillard-Kelly M, Baron R** 2002 Deletion of estrogen receptors reveals a regulatory role for estrogen receptors-β in bone remodeling in females but not in males. Bone 30:18–25
16. **Pendaries C, Darblade B, Rochaix P, Krust A, Chambon P, Korach KS, Bayard F, Arnal JF** 2002 The AF-1 activation-function of ERα may be dispensable to mediate the effect of estradiol on endothelial NO production in mice. Proc Natl Acad Sci USA 99:2205–2210
17. **Mallepell S, Krust A, Chambon P, Brisken C** 2006 Paracrine signaling through the epithelial estrogen receptor α is required for proliferation and morphogenesis in the mammary gland. Proc Natl Acad Sci USA 103:2196–2201

18. **Kos M, Denger S, Reid G, Korach KS, Gannon F** 2002 Down but not out? A novel protein isoform of the estrogen receptor α is expressed in the estrogen receptor α knockout mouse. J Mol Endocrinol 29:281–286
19. **Couse JF, Curtis SW, Washburn TF, Lindzey J, Golding TS, Lubahn DB, Smithies O, Korach KS** 1995 Analysis of transcription and estrogen insensitivity in the female mouse after targeted disruption of the estrogen receptor gene. Mol Endocrinol 9:1441–1454
20. **Risbridger G, Wang H, Young P, Kurita T, Wang YZ, Lubahn D, Gustafsson JA, Cunha G** 2001 Evidence that epithelial and mesenchymal estrogen receptor-α mediates effects of estrogen on prostatic epithelium. Dev Biol 229:432–442
21. **Ricke WA, McPherson SJ, Bianco JJ, Cunha GR, Wang Y, Risbridger GP** 2008 Prostatic hormonal carcinogenesis is mediated by *in situ* estrogen production and estrogen receptor α signaling. FASEB J 22:1512–1520
22. **Lubahn DB, Moyer JS, Golding TS, Couse JF, Korach KS, Smithies O** 1993 Alteration of reproductive function but not prenatal sexual development after insertional disruption of the mouse estrogen receptor gene. Proc Natl Acad Sci USA 90:11162–11166
23. **Feng Y, Manka D, Wagner KU, Khan SA** 2007 Estrogen receptor-α expression in the mammary epithelium is required for ductal and alveolar morphogenesis in mice. Proc Natl Acad Sci USA 104:14718–14723
24. **Chen M, Wolfe A, Wang X, Chang C, Yeh S, Radovick S,** 2008 Generation and characterization of a complete null estrogen receptor α mouse using Cre/LoxP technology. Mol Cell Biochem, [Epub ahead of print]
25. **Ni J, Wen X, Yao J, Chang HC, Yin Y, Zhang M, Xie S, Chen M, Simons B, Chang P, di Sant'Agnese A, Messing EM, Yeh S** 2005 Tocopherol-associated protein suppresses prostate cancer cell growth by inhibition of the phosphoinositide 3-kinase pathway. Cancer Res 65:9807–9816
26. **Yin Y, Ni J, Chen M, DiMaggio MA, Guo Y, Yeh S** 2007 The therapeutic and preventive effect of RRR-α-vitamin E succinate on prostate cancer via induction of insulin-like growth factor binding protein-3. Clin Cancer Res 13:2271–2280
27. **Zhang M, Altuwaijri S, Yeh S** 2004 RRR-α-tocopheryl succinate inhibits human prostate cancer cell invasiveness. Oncogene 23:3080–3088
28. **Cunha GR, Ricke W, Thomson A, Marker PC, Risbridger G, Hayward SW, Wang YZ, Donjacour AA, Kurita T** 2004 Hormonal, cellular, and molecular regulation of normal and neoplastic prostatic development. J Steroid Biochem Mol Biol 92:221–236
29. **Sugimura Y, Cunha GR, Donjacour AA** 1986 Morphogenesis of ductal networks in the mouse prostate. Biol Reprod 34:961–971
30. **Chang WY, Wilson MJ, Birch L, Prins GS** 1999 Neonatal estrogen stimulates proliferation of periductal fibroblasts and alters the extracellular matrix composition in the rat prostate. Endocrinology 140:405–415
31. **Thomson AA, Timms BG, Barton L, Cunha GR, Grace OC** 2002 The role of smooth muscle in regulating prostatic induction. Development 129:1905–1912
32. **Marker PC, Donjacour AA, Dahiya R, Cunha GR** 2003 Hormonal, cellular, and molecular control of prostatic development. Dev Biol 253:165–174
33. **Grishina IB, Kim SY, Ferrara C, Makarenkova HP, Walden PD** 2005 BMP7 inhibits branching morphogenesis in the prostate gland and interferes with Notch signaling. Dev Biol 288:334–347
34. **Lamm ML, Podlasek CA, Barnett DH, Lee J, Clemens JQ, Hebner CM, Bushman W** 2001 Mesenchymal factor bone morphogenetic protein 4 restricts ductal budding and branching morphogenesis in the developing prostate. Dev Biol 232:301–314
35. **Donjacour AA, Cunha GR** 1988 The effect of androgen deprivation on branching morphogenesis in the mouse prostate. Dev Biol 128:1–14
36. **Jarred RA, Cancilla B, Prins GS, Thayer KA, Cunha GR, Risbridger GP** 2000 Evidence that estrogens directly alter androgen-regulated prostate development. Endocrinology 141:3471–3477
37. **Singh J, Handelsman DJ** 1999 Morphometric studies of neonatal estrogen imprinting in the mature mouse prostate. J Endocrinol 162:39–48
38. **Prins GS** 1992 Neonatal estrogen exposure induces lobe-specific alterations in adult rat prostate androgen receptor expression. Endocrinology 130: 3703–3714
39. **Rajfer J, Coffey DS** 1978 Sex steroid imprinting of the immature prostate. Long-term effects. Invest Urol 16:186–190
40. **Taylor RA, Cowin P, Couse JF, Korach KS, Risbridger GP** 2006 17β-Estradiol induces apoptosis in the developing rodent prostate independently of ERα or ERβ. Endocrinology 147:191–200
41. **Timms BG, Petersen SL, vom Saal FS** 1999 Prostate gland growth during development is stimulated in both male and female rat fetuses by intrauterine proximity to female fetuses. J Urol 161:1694–1701
42. **vom Saal FS, Timms BG, Montano MM, Palanza P, Thayer KA, Nagel SC, Dhar MD, Ganjam VK, Parmigiani S, Welshons WV** 1997 Prostate enlargement in mice due to fetal exposure to low doses of estradiol or diethylstilbestrol and opposite effects at high doses. Proc Natl Acad Sci USA 94:2056–2061
43. **McPherson SJ, Ellem SJ, Simpson ER, Patchev V, Fritzemeier KH, Risbridger GP** 2007 Essential role for estrogen receptor β in stromal-epithelial regulation of prostatic hyperplasia. Endocrinology 148:566–574
44. **Prins GS, Birch L** 1997 Neonatal estrogen exposure up-regulates estrogen receptor expression in the developing and adult rat prostate lobes. Endocrinology 138:1801–1809